Advances in Nano Research, *Vol. 14, No. 2 (2023) 201-210*
https://doi.org/10.12989/anr.2023.14.2.201

Examining the performance of PAI/ZnO synthesized with diamine and nano particles

Jianwei Shi and Xiaoxu Teng*

School of Chemistry and Chemical Engineering, Yangtze Normal University, Chongqing 408100, Chongqing, China

(*Received March 25, 2022, Revised August 17, 2022, Accepted August 18, 2022*)

Abstract. A ZnO/poly (amide-imide) hybrid nanocomposite film with different weight percentages of Zinc oxide (ZnO) nanoparticles is synthesized and characterized in this paper. A two-step reaction successfully synthesized a new kind of heteroaromatic diamine with bulky pendant groups. In order to produce 3, 5-dinitro-3, 3-bis (4-(4-Nitrophenoxy) phenyl) -2-benzofuran-1-one, 3, 3'-bis (4-hydroxyphenyl) benzofuran-1-one and 3'-bis (4-hydroxyphenyl) benzofuran-1-one were combined with 3'-bis (3-hydroxyphenyl) benzofuran-1-one. The obtained dinitro was then reduced by zinc dust and hydrochloric acid. The reaction of 4, 4* carbonyl diphthalic anhydride with amino acid L-alanine in acetic acid leads to the production of very high yields of chiral diacid monomer. As a result of the direct polymerization of these monomers, new optically active polymers were formed (amide-imide). In order to synthesize poly (amide-imide)/ZnO nanocomposites with different weight percentages (2, 4, 6, 8, and 10%), PAI and ZnO nanoparticles were combined using ultrasonication SEM, Fourier transform infrared spectroscopy, X-ray diffraction and thermal gravimetry were used to characterize the PAI films.
Keywords: chiral diacid; diamine; nano composite; PAI/ZnO

1. Introduction

Recently, organic-inorganic nanocomposites have become one of the most extensively studied materials worldwide because of their unique combination of inorganic and organic properties (Granqvist 1993, Paul and Robeson 2008, Sato *et al.* 2008). Inorganic nanoparticles and organic polymer are combined to produce polymer nanocomposites moreover (Sun *et al.* 2022, Zhou *et al.* 2022). Inorganic nanoparticles embedding in polymer matrix provided high-performance novel materials for semiconductors, sensors, fuel cells, drug delivery, and rechargeable batteries (Knauth and Schoonman 2007, Lee and Kobayashi 2010, Fawaz and Mittal 2015). Due to their high volume-to-surface area ratio, nanoparticles tend to aggregate during the preparation of nanocomposites, making homogeneous scattering difficult (Li *et al.* 2022, Luo *et al.* 2022). Surface modification and silane coupling agents can overcome this problem (Elamin and Elsanousi 2013, Panutumrong *et al.* 2015). In poly (amide-imide) polymers, there is positive succor of polyamide and Polyimide properties, such as good solvent solubility, high chemical stability, and high thermal resistance (O'Donnell and Baird 1995, Mohan and Reddy 2007, Mallakpour and Madani 2012). Polymers are ideal candidates for advanced applications like separation membranes, wire enamel, sensors, adhesives, composite materials, injection molding, and extrusion products (Gornicka and Gorecki 2010, Hsiao *et al.* 2011, Omanović-Mikličanin *et al.* 2020).

Zinc oxide (ZnO) is an ecological nanoparticle with ultraviolet and infrared absorption, high luminescence, strong catalytic activity, and a high electromechanical coupling coefficient (Yu *et al.* 2018, Djahnit *et al.* 2019). The nanocomposite PAI polymer and ZnO nanoparticles have attracted great attention because they have special physical and chemical properties (Hu *et al.* 2021, Han *et al.* 2022, Yang *et al.* 2022). Integrating ZnO nanoparticles into the polymer matrix prepares higher optical, mechanical, thermal, electronic, and conductivity attributes for the resulting organic nanocomposite (these nanoparticles provide thermal stability, mechanical properties, and conductivity properties to polymers) (Meilert *et al.* 2005, Fateh *et al.* 2014). The existing study has synthesized poly (amide-imide) /ZnO hybrid optical active nanocomposites with different ZnO weight percentages (Ning *et al.* 2021, Sheng *et al.* 2021, Lu *et al.* 2022). FTIR, elemental analysis, thermogravimetric analysis (TGA), proton-nuclear magnetic resonance (NMR) spectroscopy, and proton-nuclear magnetic resonance (1H NMR) spectroscopy are also used to characterize the monomers and nanocomposite materials.

2. Result and discussion

Under a nitrogenous atmosphere, a polymerization reaction taking place at 110°C took 5 hours with NMP as a solvent and TPP as the acid activator. In optimized condensations, PAI had an intrinsic viscosity of 0.36 dl/g and showed high yields. By measuring the polymer's special rotation, the chiral unit was integrated into the polymer's backbone. These PAI/ZnO NCs have different percentages of ZnO nanoparticles (2, 4, 6, 8, and 10%). PAI

*Corresponding author, Ph.D.,
E-mail: tengxiaoxu@sina.com

ISSN: 2287-237X (Print), 2287-2388 (Online)

Table 1 Pure PAI and PAI/ZnO nanocomposites' thermal properties

Sample	PAI	PAI/4%ZnO	PAI/10%ZnO
T_5[a]	241	325	356
T_{10}[b]	293	369	392
Char Yield	33	24	23
LOI	31.2	27.7	25.5

[a] Under a nitrogen atmosphere, TGA recorded 5% weight loss at 10 °C/min heating

functional groups interact with ZnO NPs modified with hydroxyl groups for dispersion within the polymer matrix, as shown in Fig. 1, PAI, ZnO modified with KH550, and PAI/ZnO nanocomposites were investigated using FT-IR. The FT-IR spectra of the PAI, KH550-modified ZnO, and PAI/ZnO nanocomposites show amide (NH) stretching at 3415 cm-1, symmetric imide frequency (C=O) stretching at 1770 cm-1, and amide (C=O) stretching at 1616 cm-1. Stretching vibrations at 1386 and 763 cm-1 indicate imide ring, absorption bands. Stretching and bending vibrations in the 3432 cm-1 regions are associated with the -OH, -NH2 groups. Adding KH550 causes the absorbance band in the 1282 cm-1 to be attributed to Si-O groups. It is also possible to assign the peak at 876 cm-1 to the bending mode of the Si-OH group. ZnO vibration frequencies are at 447 cm-1. The absorption band Zn-O-Zn at 580 cm-1 confirms the deformation of the PAI/ZnO nanocomposite.

The X-ray diffraction results of pure PAI/ZnO nano-composites and ZnO-NPs are shown in Fig. 2, Fig. 3, and Fig. 4. Pursuant to the results, PAI possesses no sharp diffraction peaks due to its amorphous nature. XRD patterns of ZnO powder exhibited diffraction peaks corresponding to hexagonally wurtzite ZnO, which according to the JCPDS standard values for ZnO, are consistent. According to the literature, the peaks at 2h = 31.7, 35.6, 35.9, 47.3, 56.0, 62.9, 66.5, 68.0, 68.9, 72.5, and 75.2 correspond to nano-ZnO peaks (1 0 0), (0 0 2), (1 0 1), (1 0 2), (1 1 0), (1 0 3), (1 1 2), (2 0 0), (2 0 1), (0 0 4) and (2 0 2).

A TGA curve is shown in Fig. 5 for a PAI and PAI/ZnO nanocomposite with a weight percentage of 4 and 10%, respectively. The thermal stability of polymers and residues was studied at 800 0C (char yield) based on weight loss of 4 and 10 percent (T5, T10). TGA reported that PAI is thermally stable at 210 degrees Celsius. In Table 1, we summarize the TGA results for pure PAI and nanocomposites. An equation from Van Krevelen and Hoftyzer determines the LOI value (Yu *et al.* 2018).

$$LOI = 17/5+4/0\ CR \quad (1)$$

where CR = char yield. Relative to PAI/ZnO nano-composites, pure PAI exhibits a higher polymer decomposition temperature. With increasing nanoparticle content (percentage), thermal stability also increased. Based on the LOI value of nanocomposites (4 and 10 weight %), as shown in Table 1, they belong to the class of self-extinguishing nanocomposite polymers.

An FE-SEM micrograph of a PAI/ZnO nanocomposite (10 wt %) is shown in Fig. 6. Surface modification of nanoparticles decreases their surface energy and decreases particle aggregation. During the photographing, there is no evidence of particle aggregation. ZnO-NPs were observed in the PAI matrix with homogeneous dispersion. (the mean size of the particles is 40 nm).

3. Experimental data

3.1 Materials

Merck Chemical Co, Fluka Chemical Co (Buchs, Switzerland), and Aldrich Chemical Co (Milwaukee, WI) supplied analytical-grade chemicals and solvents. Zinc acetate dehydrates (Zn (CH3COO)22H2O) were purchased from Aldrich Chemical Company. BTDA, from Merck, was reconstituted from acetic anhydride before use. Triphenyl phosphite (TPP), tetrabutylammonium bromide (TBAB), and L- alanine were procurement from Merck.

3.2 Measurements

In the presence of KBr, we recorded FT-IR spectra using a spectrophotometer (Jasco-680, Japan). By using 1 mg of sample in 100 mg KBr, the FTIR spectrum of the samples was modified by 400-4000 cm-1. For all 1H-NMR spectra, a 250 MHz Bruker Ultrashelled NMR device was used, and dimethyl sulfoxide (DMSO-d6) was used as the solvent. X-ray scattering measurement of compounds with X-ray diffraction spectrometer (XRD) Philips X'PERT MPD model in the range of 2θ, 20–900 degrees with Cu Kα λ = 1.54 Å with a scanning speed of 0.050/min, under acceleration 35kV/40 mA beam was performed. KYKY-EM320 was used to analyze scanning electron microscope (FE-SEM, HITACHI S-4160) data. Thermal gravimetric analysis of polymers was recorded by STA503 Win TA 10 device under nitrogen and argon atmosphere with a scanning speed of 20°C/min.

3.3 Preparation of ZnO nanoparticles

2.1 gr (0.01mol) Zn (AC) 2.2H2O and 0.84gr (0.012 mol) oxalic acid were mixed together in a Chinese cruise. After 30 minutes of drying at 450°C, the precipitate was found to be white.

3.4 Nanoparticles of ZnO with surface correction

It was stirred for 24 hours with 20 ml of toluene added to 0.1 g of ZnO and 20% by weight (0.042 ml) of KH550 added. The precipitate was thoroughly washed with toluene and acetone after filtration. A temperature of 60°C was used for 24 hours to dry the product.

3.5 Preparation of chiral diacid

3.5.1 (N, N' carbonyldiphthaloyl) bis L-alanine

In a round-bottomed flask of 25 ml, 4,4-carbonyl-diphthalic anhydride and 0.06 g (0.65 mmol) of L-alanine have been added along with 2 ml of dry acetic acid. Five

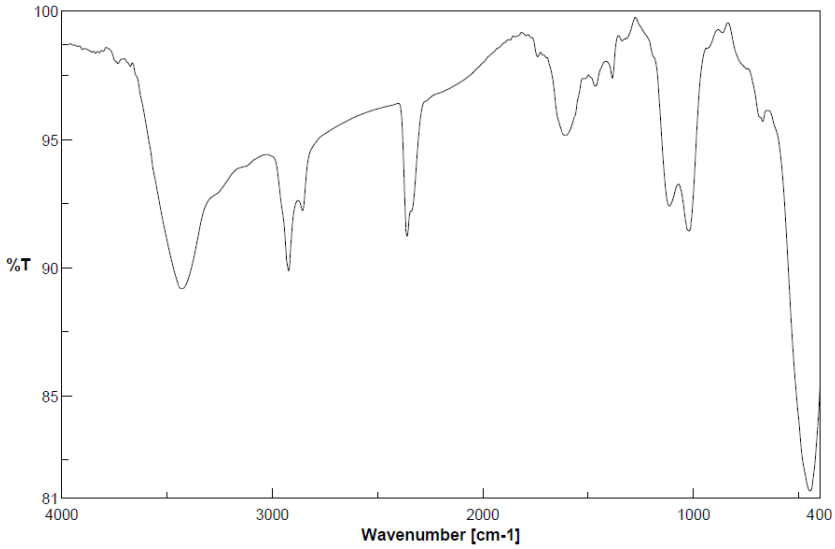

Fig. 1 FT-IR spectrum of KH550-modified ZnO

hours were spent stirring the mixture at room temperature. Six-hour reflux at 110°C was then performed. In this case, we added 10 ml of distilled water and 30 ml of hydrochloric acid to the contents of the flask after it had cooled. Compound 3 (Scheme 1), which has a melting point of 241-245°C and an 80% yield, was produced by filtering the white precipitate.

3.5.2 3, 3 –bis (4-(4-nitrophenoxy) phenyl) -2-benzofuran-1-one

At 30 °C, 0.1 g phenolphthalein and 0.14 g p-bromonitrobenzene were stirred for 10 minutes in DMF (8 mL). After adding 0.13 g of potassium bicarbonate, it was ultrasonicated for 15 minutes and refluxed at 120 °C. The mixture was cooled and stirred at room temperature for 2 hours with 10 ml of HCl. Following filtering, distilled water was used to wash and dry the yellow precipitate obtained.

3.5.3 3, 3'-bis (4-(4-aminophenoxy) phenyl) -2-benzofuran-1-one

The dinitro compound 3,3-bis(4-nitrophenoxy) phenyl)-2-benzofuran-1-one was dissolved in 0.4 mL of hydrochloric acid (d. 1.18) at a concentration of 0.1 g. The reaction mixture was stirred at room temperature for 20 minutes, followed by 0.4 ml of water. After refluxing for an hour at 90°C, 0.107 g of zinc powder was added. The precipitate formed after cooling was filtered and made alkaline with 10% sodium hydroxide. After removing the solvent, 0.08 g (80%) of milky crystals with a melting point of 275-279 °C were formed. (Scheme 2).

3.6 The preparation of poly(amide-imide)s with optical properties

In a 25 mL flask, chiral PAI (Scheme 3) was prepared by combining 0.10 g of the diacid, 0.11 g of the diamine, 0.22 mL of TPP, and 0.5 mL NMP as the solvent, 0.06 g of CaCl2, and 0.15 mL pyridine. Under nitrogen gas, 110 °C was refluxed for five hours under a nitrogen atmosphere. A viscous mixture was obtained by stirring 30 ml of methanol into the mixture for three hours after cooling. The brown solid was filtered and dried to yield 0.11 g (77%) of PAI, mp 3040°C.

3.7 Poly (amide-imide)/ZnO nanocomposite film synthesis

PAI/ZnO NCs were prepared by dispersing 0.2 grams of PAI in 30 ml of ethanol under ultrasonic irradiation for 20 minutes, followed by adding Nanoparticles of modified ZnO (2, 4, 6, 8, and 10% W/W) and ultrasonically agitating for 4 hours. A vacuum drying process at 80 0C for 24 hours was performed after the nanocomposites were irradiated and the solvent was removed.

4. Conclusions

According to the TGA results, PAI/ZnO nanocomposites containing zinc oxide nanoparticles in their matrix exhibit greater thermal resistance than pure polymer composites under ultrasonic irradiation. PAI has been loaded with ZnO nanoparticles according to SEM images. The presence of nanoparticles in PAI films was confirmed by X-ray diffraction. A strong attraction between PAI and ZnO nanoparticles was also demonstrated by FTIR studies.

5. Supporting Information

5.1 Characterization of ZnO nanoparticle

In Fig. 1, we observed the FT-IR spectrum of ZnO nanoparticles. Bonds between Zn and O are characterized by peaks at 438 cm-1. In accordance with the covalent bonding between ZnO NPs and KH550, the characteristic peaks at 3432 cm-1 (–OH), 2923 cm-1 (-CH2 stretching), and 1287 cm-1 (SiOH) and 876 cm-1 (Zn–O–Si) were

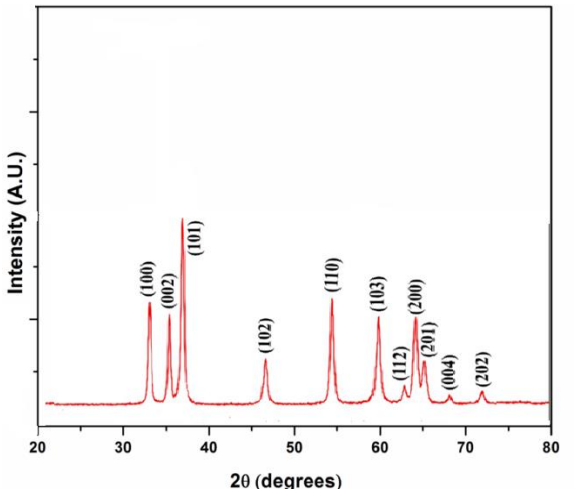

Fig. 2 ZnO nanoparticles X-rayed

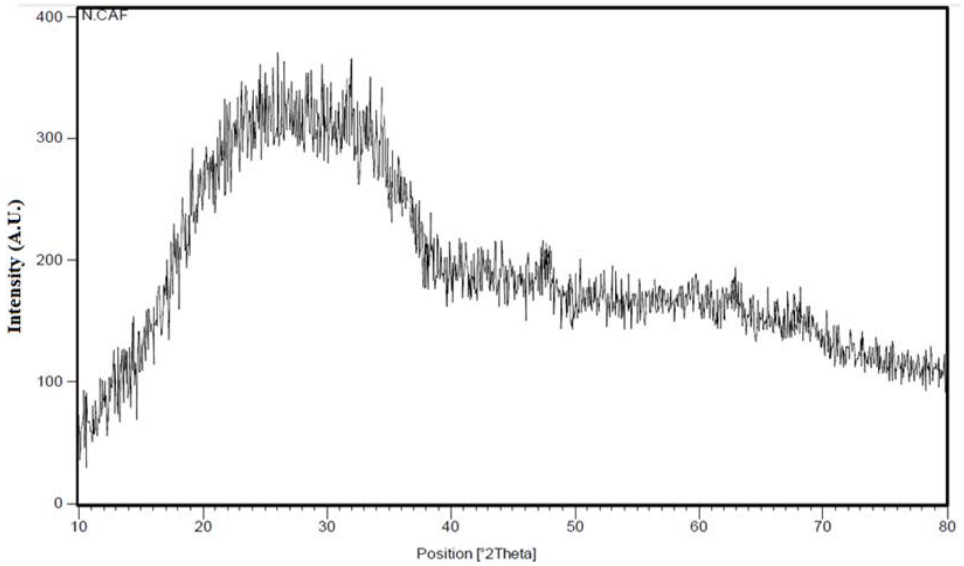

Fig. 3 The X-ray PAI

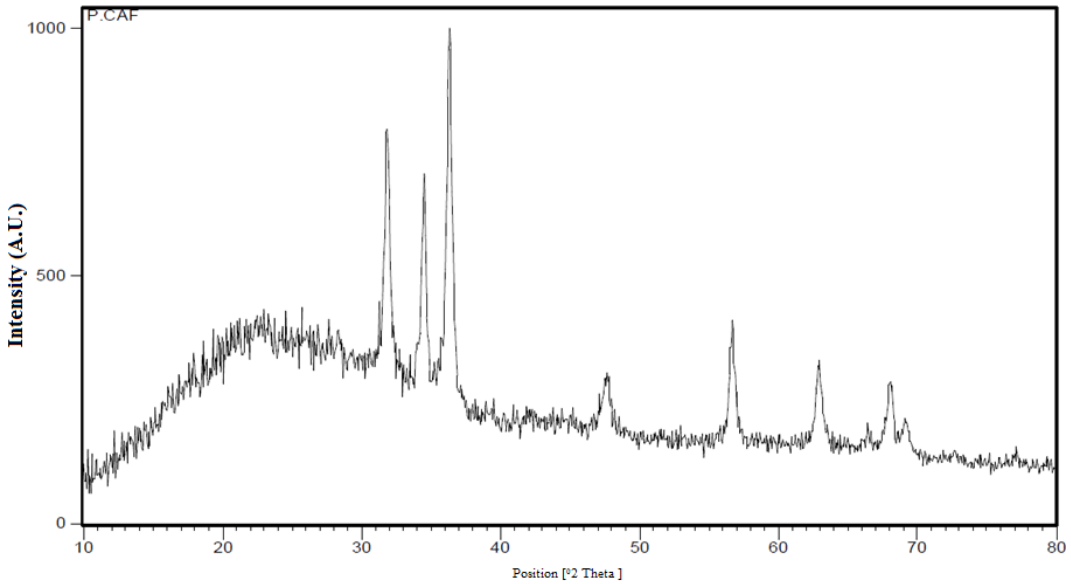

Fig. 4 The X-ray PAI/ZnO 10 wt% nanocomposite

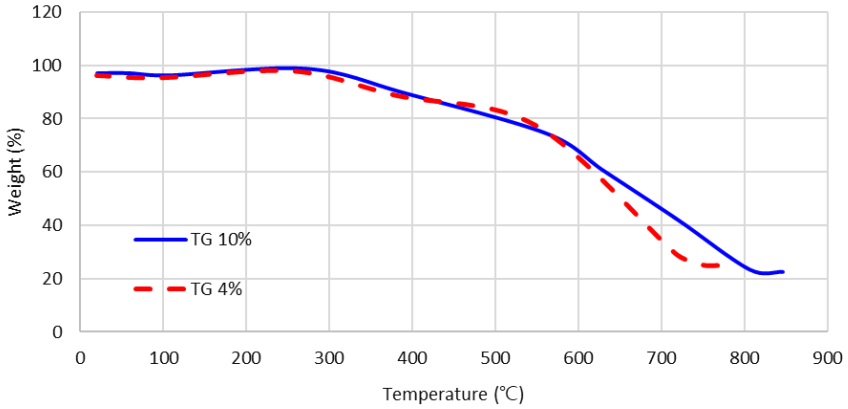

Fig. 5 The properties of PAI/ZnO nanocomposites in TGA (4 and 10 wt %)

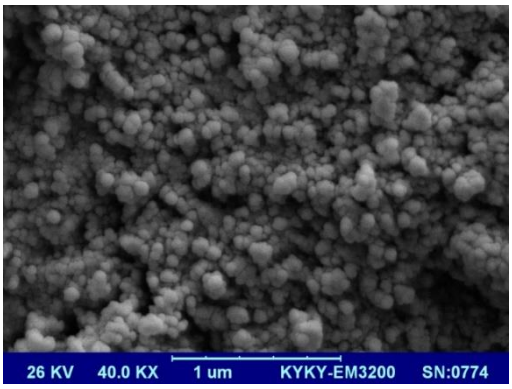

Fig. 6 Nanocomposite PAI/ZnO 10 wt% imaged by FE-SEM

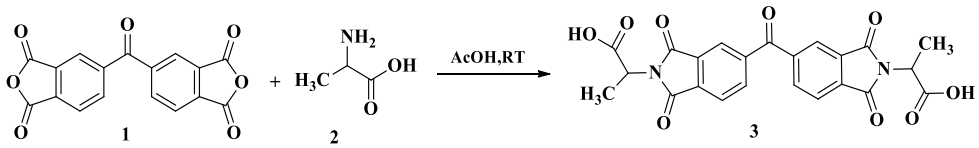

Scheme 1 A method for synthesis of chiral diacid

obtained. All those bands showed that silane groups were graphed on the surface of the ZnO NRs.

In Fig. 2, the XRD model, ZnO, all peaks in X-ray diffraction well represent the hexagonal structure of ZnO vertexite, where the maximum intensity peak is shown on page 101 at 2 36/5 angles.

5.2 Experimental section

5.2.1 Creating PAI/ZnO NC films: general procedure

We added the diamine to the synthesized diacid, then dried calcium chloride, triphenyl phosphate, NMP, and pyridine to the mixture, and then slowly refluxed it at 110 °C for five hours under nitrogen pressure. With a magnetic stirrer, the mixture was stirred in a room for three hours after the viscous site became less viscous. Following the precipitate's washing and drying, it was washed with hot water. Mixtures of ZnO modified with KH550 in proportions of 2, 4, 6, 8, and 10 were ultrasound for four hours with dry ethanol to obtain a polymer (amide-imide). It was then removed from the solvent and baked for two hours at 80°C.

5.2.2 IR., 1H NMR spectrum, and C. H. N analyses of compounds

5.2.2.1 3, 3-bis (4-(4-nitrophenoxy) phenyl) -2-benzofuran-1-one

Yellow needle crystal, M.P.: 256 °C, decompose. IR (KBr) (νmax/cm−1): 1471, 1595 (C=C, Ar), 1504, 1346 (NO2), 1238, 1110 (C-O-C), 3051 (C–H, sp2stretch) (Fig. 7).

1H NMR: 6.3 (d, 4H, j = 6 Hz), 7.78–7.8 (dd, 4H), 6.9 (d, 4H), 8.3 (d, 1H), 7.1 (d, 4H), 8.1 (d, 1H, j = 8 Hz), 7.6 (d, 1H, j = 7 Hz), (400 MHz, DMSO-d6) δ (ppm) (Fig. 8).

5.2.2.2 3, 3-bis (4-(4-aminophenoxy) phenyl) -2-benzofuran-1-one

Milky needle crystal, 1585, 1486 (C=C, Ar), 1338 (N-C), 1108, 1249 (C-O-C), 1776 (O=C), 2977 3295, 3486, 3494 (NH, NH2), (H–C, sp2stretch), decompose. IR (KBr) (vmax/cm−1), M.P: 279 °C (Fig. 9).

1H NMR: 7.9 (d, 2H), 4.6 (s, 4H, j = 4 Hz), 7.3 (d, 4H), 7.4 (d, 4H, j = 7 Hz), 7.2 (d, 4H), 7.7–7.9 (dd, 4H, j = 4 Hz), 7.6 (d, 1H, j = 7 Hz), 7.8 (d, 1H), (400 MHz),(DMSO-d6) δ (ppm) (Fig. 10).

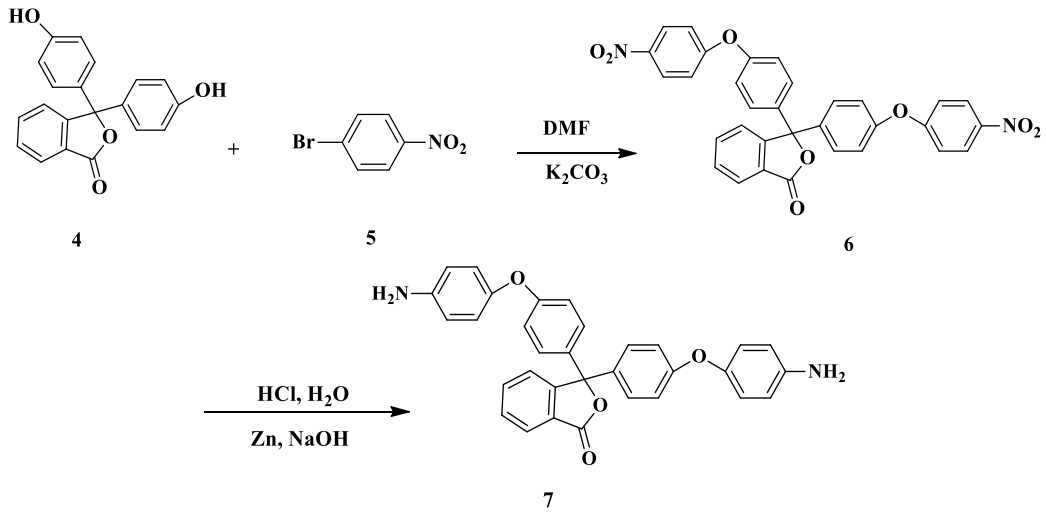

Scheme 2 A synthesis of diamine

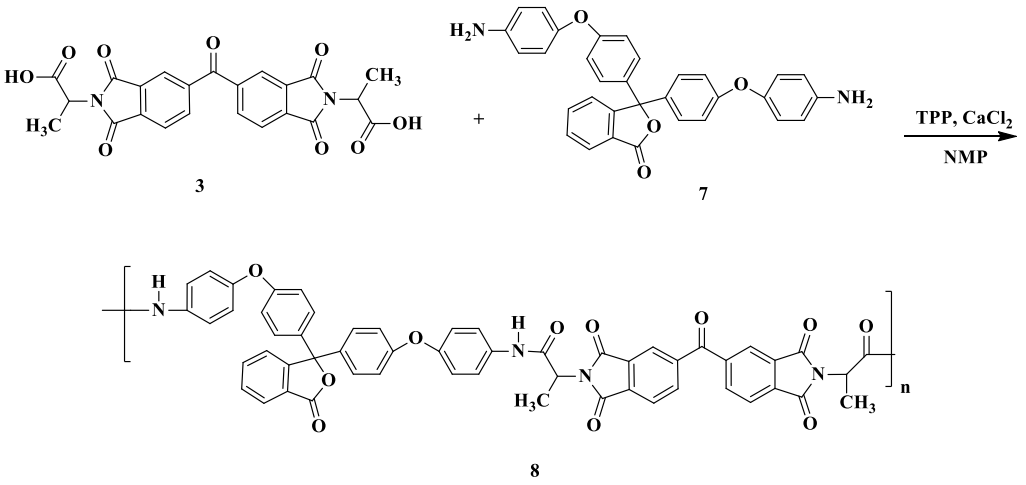

Scheme 3 Preparation of PAI

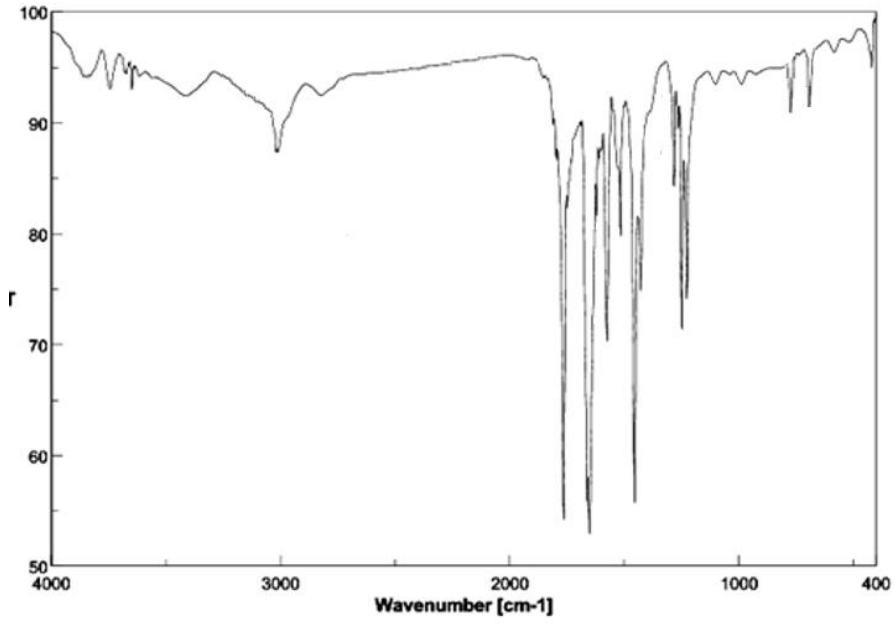

Fig. 7 Spectral analysis from compound 6 using FT-IR

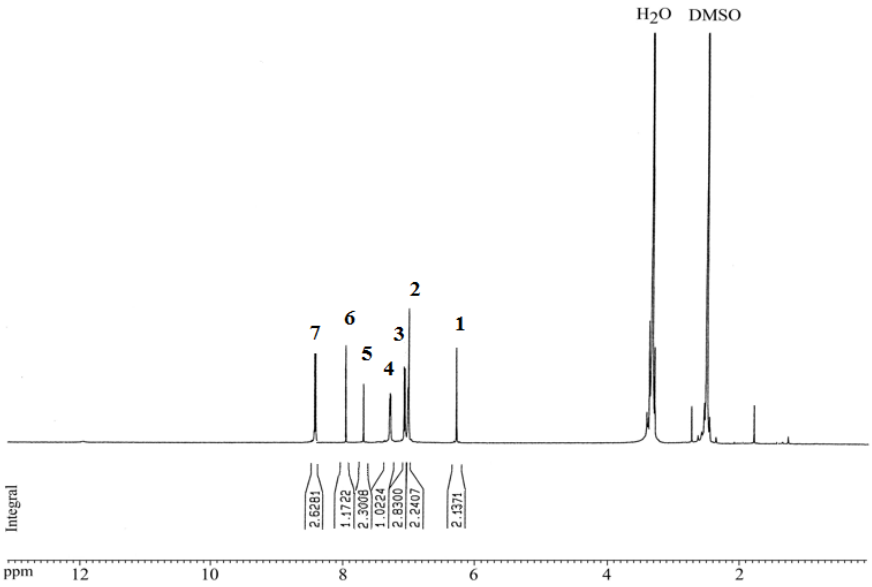

Fig. 8 Spectral analysis from compound 6 using HNMR

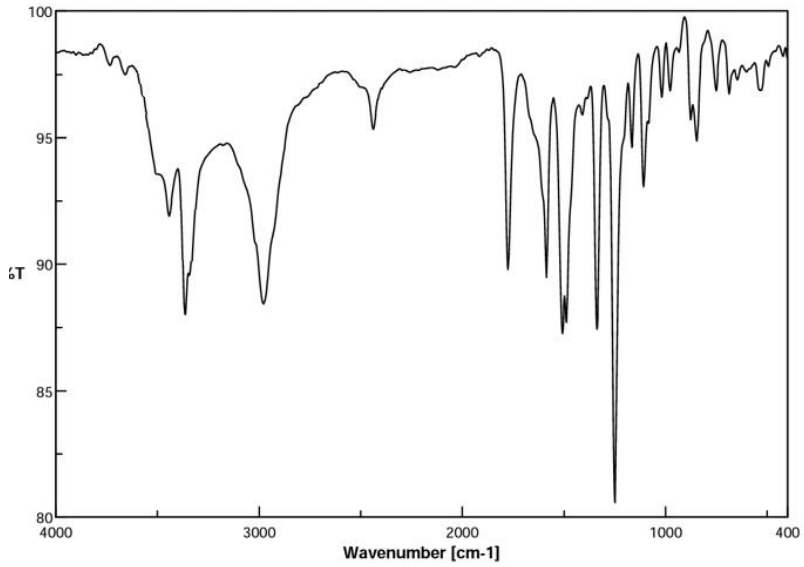

Fig. 9 Spectral analysis from compound 7 using FT-IR

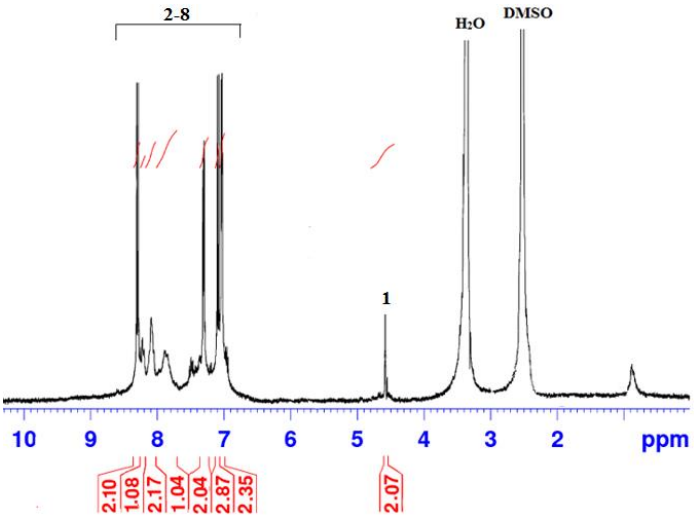

Fig. 10 Spectral analysis from compound 7 using HNMR

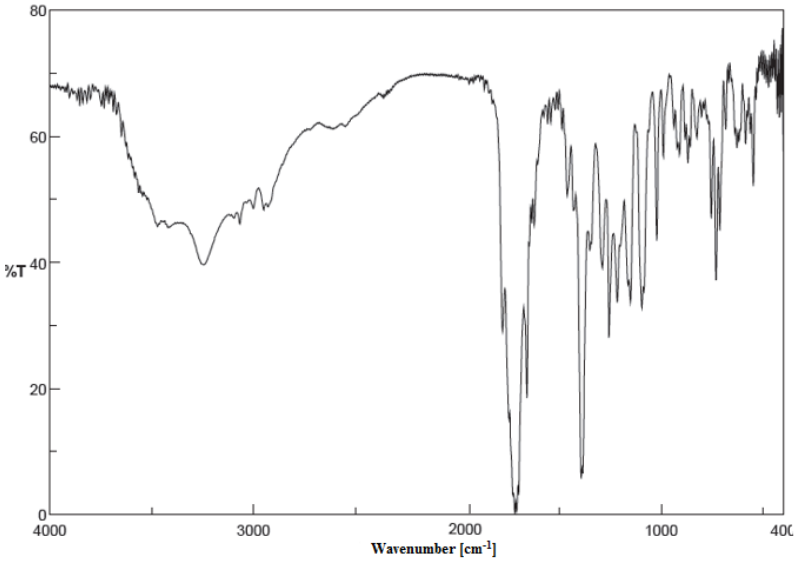

Fig. 11 Spectral analysis from compound 3 using FT-IR

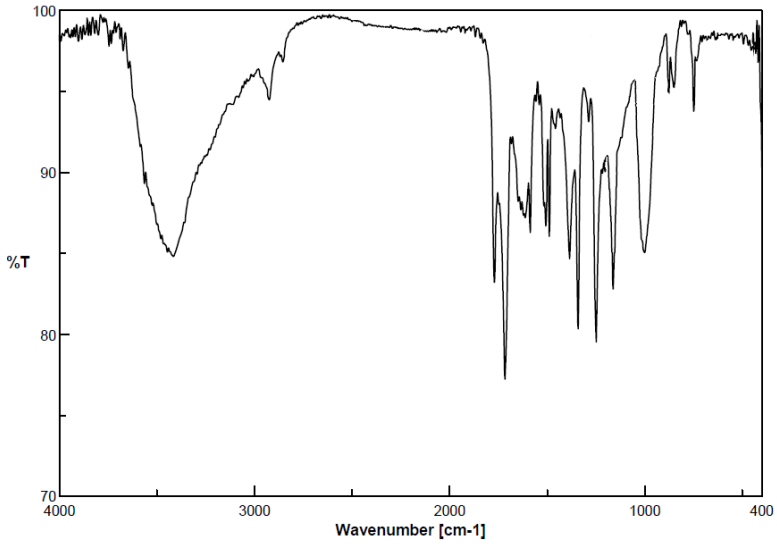

Fig. 12 Spectral analysis from PAI using FT-IR

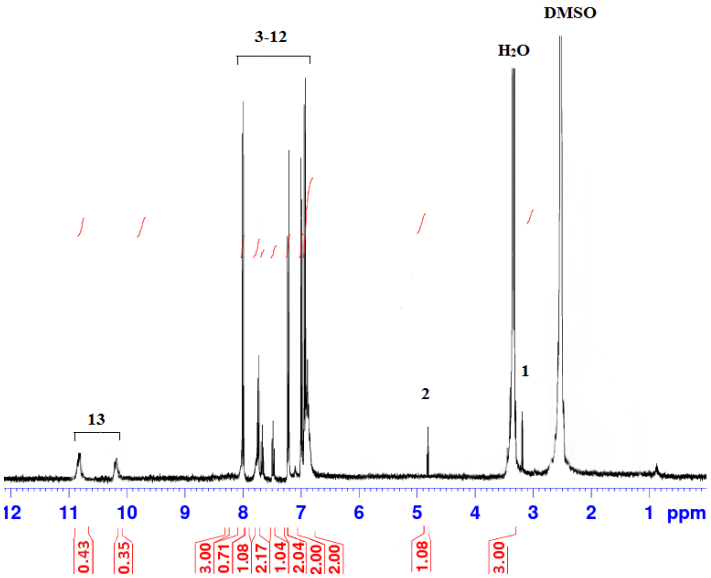

Fig. 13 Spectral analysis from PAI using HNMR

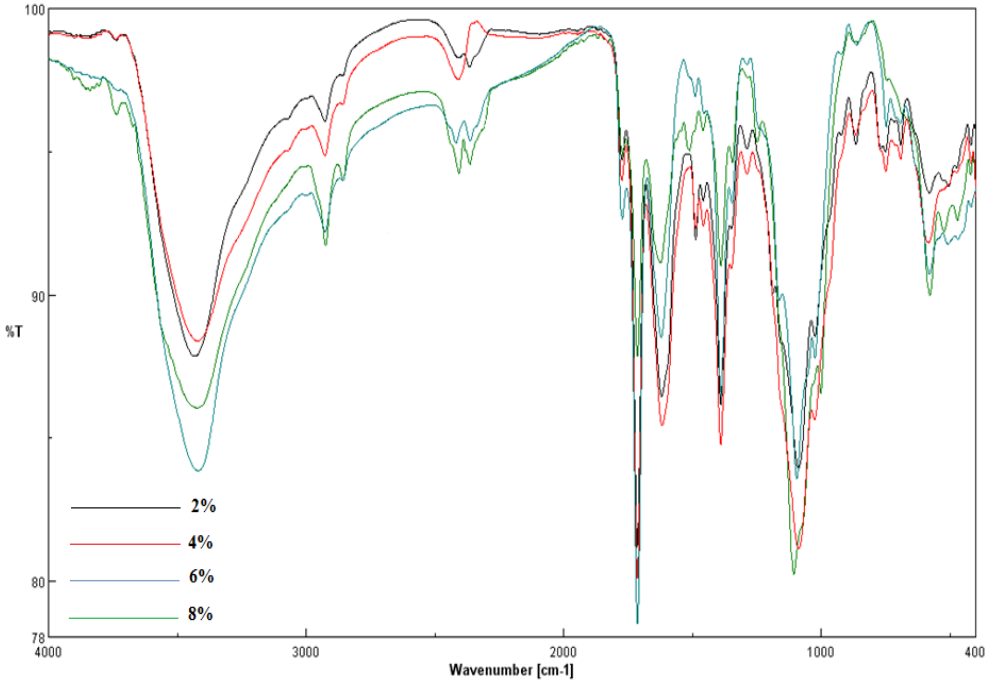

Fig. 14 Spectral analysis from PAI/ZnO using FT-IR

5.2.2.3 4, 4'-Carbonyl-bis (phthaloyl-L-alanine)

White needle crystal, M.P: 243 °C, decompose: 1712(symmetrical O=C, imide stretch), 1621(O=C), 1481(C-N stretch), 3409(H-O stretch), 1778(asymmetrical O=C, imide stretch), 3058(aromatic C-H stretch), 2929(aliphatic H-C stretch), and 726 (imide ring deformation), IR (KBr) (νmax/cm−1)(Fig. 11).

5.2.2.4 Poly (amide-imide)

Brown needle crystal: 3415 (NH), 1472, 1509 (C=C, Ar), 1103, 1250 (C-O-C), 1716 (C=O imide), 1350 (C-N), 2925 (C–H, sp2stretch), 1770, IR (KBr) (νmax/cm−1), M.P: 304 °C, decompose (Fig. 12).

1H NMR: 3.32 (d, 6H), 7.92 (d, 2H, j = 2.1 Hz), 8.14–8.2 (m, 6H, j = 4 Hz), 4.92 (q, 2H), 7.39 (d, 4H), 7.66–7.7 (dd, 4H, j = 4 Hz), 7.48 (d, 4H, j = 7 Hz), 7.86 (d, 2H), 7.58(d, 4H, j), 10.3 (s, 1H), 10.91 (s, 1H), (400 MHz), (DMSO-d6) δ (ppm) (Fig. 13).

5.2.2.5 ZnO nanoparticle

White powder. IR (KBr) (νmax/cm−1): 3432 (OH), 438 (Zn-O).

5.2.2.6 Modification of ZnO nanoparticles

White powder: 2925, 2360(C-H stretch), 1282(Si-O bond), 3432(H-O and H-N stretch), 876 (bending mode Si–O.H.), 447(Zn-O stretch), I.R. (νmax/cm−1) (KBr) (Fig. 14).

Acknowledgement

This work was supported by the National Natural Science Foundation of China (21808017), the Science and Technology Research Project of Chongqing Education Board (CXQT21037 and KJQN201901428) and Fuling Science and Technology Commission Project (FLKJ, 2021ABB1041). The Natural Science Foundation Project of Chongqing CSTC (2022NSCQ-MSX0304).

References

Djahnit, L., Sened, N., El-Miloudi, K., Lopez-Manchado, M.A. and Haddaoui, N. (2019), "Structural characterization and thermal degradation of poly (methylmethacrylate)/zinc oxide nanocomposites", *J. Macromol. Sci. A*, **56**(3), 189-196. https://doi.org/10.1080/10601325.2018.1563494.

Elamin, N. and Elsanousi, A. (2013), "Synthesis of ZnO nanostructures and their photocatalytic activity", *J. Appl. Ind. Sci.*, **1**(1), 32-35.

Fateh, R., Dillert, R. and Bahnemann, D. (2014), "Self-cleaning properties, mechanical stability, and adhesion strength of transparent photocatalytic TiO2–ZnO coatings on polycarbonate", *ACS Appl. Mater. Interf.*, **6**(4), 2270-2278. https://doi.org/10.1021/am4051876.

Fawaz, J. and Mittal, V. (2015), "Synthesis of polymer nanocomposites: review of various techniques", *Synth. Tech. Polym. Nanocompos.*, 1-30. https://doi.org/10.1002/9783527670307.ch1.

Gornicka, B. and Gorecki, L. (2010), "TGA/DTG/DSC investigation of thermal ageing effects on polyamide–imide enamel", *J. Therm. Anal. Calorim.*, **101**(2), 647-650. https://doi.org/10.1007/s10973-010-0883-9.

Granqvist, C.G. (1993), "Transparent conductive electrodes for electrochromic devices: A review", *Appl. Phys. A*, **57**(1), 19-24. https://doi.org/10.1007/BF00331211

Han, M.C., He, H.W., Kong, W.K., Dong, K., Wang, B.Y., Yan, X., Wang, L.M. and Ning, X. (2022), "High-performance electret and antibacterial polypropylene meltblown nonwoven materials doped with boehmite and ZnO nanoparticles for air filtration", *Fiber Polym.*, **23**(7), 1947-1955. https://doi.org/10.1007/s12221-022-4786-8.

Hsiao, S.H., Guo, W., Kung, Y.C. and Lee, Y.J. (2011), "Redox-active and electrochromic aromatic poly (amide-imide) s with 2, 4-dimethoxytriphenylamine chromophores", *J. Polym. Res.*, **18**(6), 1353-1364. https://doi.org/10.1007/s10965-010-9538-6.

Hu, L.B., Huang, X.Y., Zhang, S., Chen, X., Dong, X.H., Jin, H., Jiang, Z.Y., Gong, X.R., Xie, Y.X., Li, C., Chi, Z.T. and Xie, W.F. (2021), "MoO3 structures transition from nanoflowers to nanorods and their sensing performances", *J. Mater. Sci. Mater. Electron.*, **32**(19), 23728-23736. https://doi.org/10.1007/s10854-021-06464-7.

Knauth, P. and Schoonman, J. (2007), *Nanocomposites: Ionic Conducting Materials and Structural Spectroscopies*, Springer Science & Business Media.

Lee, K.S. and Kobayashi, S. (2010), *Polymer Materials: Block-Copolymers, Nanocomposites, Organic/Inorganic Hybrids, Polymethylenes*, Springer.

Li, T., Yin, W., Gao, S., Sun, Y., Xu, P., Wu, S., Kong, H., Yang, G. and Wei, G. (2022), "The combination of two-dimensional nanomaterials with metal oxide nanoparticles for gas sensors: A review", *Nanomaterials*, **12**(6). https://doi.org/10.3390/nano12060982.

Lu, T., Yan, W., Feng, G., Luo, X., Hu, Y., Guo, J., Yu, Z., Zhao, Z. and Ding, S. (2022), "Singlet oxygen-promoted one-pot synthesis of highly ordered mesoporous silica materials via the radical route", *Green Chem.*, **24**(12), 4778-4782. https://doi.org/10.1039/D2GC00869F.

Luo, Y., Xie, Y., Geng, W., Chu, J., Wu, H., Xie, D., Sheng, X. and Mei, Y. (2022), "Boosting fire safety and mechanical performance of thermoplastic polyurethane by the face-to-face two-dimensional phosphorene/MXene architecture", *J. Mater. Sci. Technol.*, **129**, 27-39. https://doi.org/10.1016/j.jmst.2022.05.003.

Mallakpour, S. and Madani, M. (2012), "Use of silane coupling agent for surface modification of zinc oxide as inorganic filler and preparation of poly (amide-imide)/zinc oxide nano-composite containing phenylalanine moieties", *Bull. Mater. Sci.*, **35**(3), 333-339. https://doi.org/10.1007/s12034-012-0304-8.

Meilert, K.T., Laub, D. and Kiwi, J. (2005), "Photocatalytic self-cleaning of modified cotton textiles by TiO2 clusters attached by chemical spacers", *J. Mol. Catal. A Chem.*, **237**(1-2), 101-108. https://doi.org/10.1016/j.molcata.2005.03.040.

Mohan, D.J. and Reddy, A.V.R. (2007), "Synthesis, characterization, and investigation of structure-thermal cycloimidization relationship of novel poly (amide amic acid) s to poly (amide imide) s by thermogravimetric analysis", *J. Polym. Sci. Part B*, **45**(21), 2937-2947. https://doi.org/10.1002/polb.21205.

Ning, F., He, G., Sheng, C., He, H., Wang, J., Zhou, R. and Ning, X. (2021), "Yarn on yarn abrasion performance of high modulus polyethylene fiber improved by graphene/polyurethane composites coating", *J. Eng. Fiber Fabr.*, **16**, 1558925020983563. https://doi.org/10.1177/1558925020983563.

O'Donnell, H.J. and Baird, D.G. (1995), "In situ reinforcement of polypropylene with liquid-crystalline polymers: effect of maleic anhydride-grafted polypropylene", *Polymer*, **36**(16), 3113-3126. https://doi.org/10.1016/0032-3861(95)97874-F.

Omanović-Mikličanin, E., Badnjević, A., Kazlagić, A. and Hajlovac, M. (2020), "Nanocomposites: A brief review", *Health Technol.*, **10**(1), 51-59.

Panutumrong, P., Metanawin, T. and Metanawin, S. (2015), "The effect of nano-Zinc oxide on the self-cleaning properties of cotton fabrics for textile application", *Int. J. Adv. Culture Technol.*, **3**(1), 13-20. https://doi.org/10.17703/IJACT.2015.3.1.13.

Paul, D.R. and Robeson, L.M. (2008), "Polymer nanotechnology: Nanocomposites", *Polymer*, **49**(15), 3187-3204. https://doi.org/10.1016/j.polymer.2008.04.017.

Sato, M., Kawata, A., Morito, S., Sato, Y. and Yamaguchi, I. (2008), "Preparation and properties of polymer/zinc oxide nanocomposites using functionalized zinc oxide quantum dots", *Eur. Polym. J.*, **44**(11), 3430-3438. https://doi.org/10.1016/j.eurpolymj.2008.08.014.

Sheng, C., He, G., Hu, Z., Chou, C., Shi, J., Li, J., Meng, Q., Ning, X., Wang, L. and Ning, F. (2021), "Yarn on yarn abrasion failure mechanism of ultrahigh molecular weight polyethylene fiber", *J. Eng. Fiber Fabr.*, **16**, 15589250211052766. https://doi.org/10.1177/15589250211052766.

Sun, D., Huo, J., Chen, H., Dong, Z. and Ren, R. (2022), "Experimental study of fretting fatigue in dovetail assembly considering temperature effect based on damage mechanics method", *Eng. Fail. Anal.*, **131**, 105812. https://doi.org/10.1016/j.engfailanal.2021.105812.

Yang, Y., Wang, Y., Zheng, C., Lin, H., Xu, R., Zhu, H., Bao, L. and Xu, X. (2022), "Lanthanum carbonate grafted ZSM-5 for superior phosphate uptake: Investigation of the growth and adsorption mechanism", *Chem. Eng. J.*, **430**, 133166. https://doi.org/10.1016/j.cej.2021.133166.

Yu, Q., Lin, R., Jiang, L., Wan, J. and Chen, C. (2018), "Fabrication and photocatalysis of ZnO nanotubes on transparent conductive graphene-based flexible substrates", *Sci. China Mater.*, **61**(7), 1007-1011. https://doi.org/10.1007/s40843-017-9211-9.

Zhou, J., Bai, J. and Liu, Y. (2022), "Fabrication and modeling of matching system for air-coupled transducer", *Micromachines*, **13**(5). https://doi.org/10.3390/mi13050781.

JL